Journal of Testing and Evaluation

doi:10.1520/JTE20190486 / Vol. 48 / No. 3 / 2020 / available online at www.astm.org

Eyoab Zegeye Teshale,[1] Kyle Hoegh,[2] Shongtao Dai,[2] Richard Giessel,[3] and Curt Turgeon[2]

Ground Penetrating Radar Sensitivity to Marginal Changes in Asphalt Mixture Composition

Reference

E. Zegeye Teshale, K. Hoegh, S. Dai, R. Giessel, and C. Turgeon, "Ground Penetrating Radar Sensitivity to Marginal Changes in Asphalt Mixture Composition," *Journal of Testing and Evaluation* 48, no. 3 (May/June 2020): 2295–2310. https://doi.org/10.1520/JTE20190486

ABSTRACT

Ground penetrating radar (GPR) is gaining renewed attention from many state highway agencies because of its promising application prospects for rapid, full-coverage, continuous, and nondestructive measurements of the density in newly constructed asphalt pavements. However, several operational and technical issues need to be addressed before this technology can be efficiently deployed for quality control/quality assurance practices. The operation-related challenges are relatively easily addressed with proper project-specific management practices. The technical ones, on the other hand, require improvements to the testing devices and procedures and strategic investigations for further understanding of the relationship between the GPR-measured dielectrics and the density of asphalt mixtures. The latter is particularly crucial given the production and construction variability of asphalt mixtures and the accepted practices of field adjustments to mix designs. This study investigated the sensitivity of dielectric measurements to changes in mix composition and assessed the appropriateness (or lack thereof) of using a single dielectric-density transfer model to analyze field data measured on multiple production days. The study examined asphalt mixtures designed and manufactured in the laboratory with varying amounts of limestone, a high-dielectric aggregate source, as well as plant-produced asphalt mixtures collected on multiple production days. The findings indicated that the source/composition of the aggregate structure affected density-dielectric relationships of asphalt mixtures considerably. On the contrary, the relationship appeared to be less sensitive to normal asphalt production variability (day to day variations) as long as the aggregate source proportions were maintained intact. The experimental investigation proposed in this study can be easily employed to determine the proper amount of calibration models or the extent of allowable adjustment to the mix design for asphalt pavement construction projects.

Manuscript received June 6, 2019; accepted for publication December 3, 2019; published online February 13, 2020. Issue published May 1, 2020.

[1] Office of Materials and Road Research, Minnesota Department of Transportation, 1400 Gervais Ave., MS 645, Maplewood, MN 55109, USA (Corresponding author), e-mail: eyoab.zegeye.teshale@state.mn.us, https://orcid.org/0000-0001-5914-789X

[2] Office of Materials and Road Research, Minnesota Department of Transportation, 1400 Gervais Ave., MS 645, Maplewood, MN 55109, USA

[3] Statewide Materials Service Team, Alaska Department of Transportation and Public Facilities, 5800 E. Tudor Rd., Anchorage, AK 99507, USA

Keywords

ground penetrating radar, pavement compaction evaluation, quality control, quality assurance, hot asphalt mixture, limestone, nondestructive pavement evaluation

Introduction

Achieving adequate in-place density (compaction) in newly constructed asphalt pavements is essential to ensure lasting performance and durability. Well-compacted pavements are likely to possess lower air voids, higher strength and stiffness, as well as superior resistance to fatigue and moisture-related damages. Lower air voids, in turn, are expected to slow the oxidation rate of the pavement surface and the hardening and embrittlement of the asphalt binder component, all of which provide fertile grounds for non–load-associated pavement distresses such as thermal cracking, reflective cracking, and ravelling.[1] Numerous research studies have observed that a 1 % increase above 7 % of in-place air voids would result in double-digit percentage reductions of pavement service life, fatigue performance, and resistance to rutting.[2–6] On the other hand, over-compaction to less than 2 % air voids is also shown to adversely affect the quality of pavements and to lead to asphalt bleeding and crushing of aggregates.[7] Optimal pavement performance and durability are generally observed for compaction levels ranging from 2 to 7 % in-place air voids.[8] For these reasons, state highway agencies (SHAs) have generally devoted considerable attention to the process of measuring and evaluating the compaction level of newly constructed pavements.

Traditionally, most SHAs have relied on density measurements taken from limited locations (spot tests) and statistical analysis techniques for quality control and quality assurance (QC/QA) of asphalt pavement constructions. Spot tests are expensive, time consuming, destructive (i.e., core drilling), and require certified personnel (i.e., nuclear density gage). Core drilling does not provide real-time feedback that would be useful for rapid control and remedy of density-deficient areas and is inefficient at capturing segregation (material, temperature, and compaction), which is the primary cause of early pavement failures. Given the inhomogeneous nature of asphalt mixtures and the complex production, placement, and compaction procedures, spot tests are poorly equipped to estimate the compaction level of an entire project.[7]

Many SHAs are also exploring advanced pavement design and construction technologies aimed at improving pavement compaction quality. Some of these initiatives include optimizing the compaction efforts by employing intelligent compaction technologies,[7,9] requiring improved joint construction practices and introducing new mix design optimization efforts aimed at minimizing the gap between the density achieved in the field compaction and the target density established in laboratory. These improvements are undoubtedly improving the quality of pavement compaction and reducing workmanship-related issues. However, without proper tools for measuring in-place density over the extent of the entire paved sections, it remains challenging to realize the full benefit and potential of these improvements.

In response to limitations posed by spot test methods, several researchers and manufacturers have been developing nondestructive, real-time, and continuous in-place density testing methods for the evaluation of pavement compaction during construction. The ground penetrating radar (GPR) is one of such methods used to measure the in-place density of asphalt pavements. GPR has been evolving gradually and showing great potential.[10–15] In 2015, as part of the Strategic Highway Research Program 2 (SHRP2) solutions research implementation efforts, a smaller-size dipole-type antenna systems, referred to as GSSI's PaveScan system, was specifically manufactured and introduced for QC/QA of asphalt pavement constructions.[16] The system has since found considerable interest among SHAs (i.e., Alaska, Maine, Minnesota, Texas) for full-scale mixture compaction density evaluation of newly paved pavements, and potential QC/QA applications. The system is referred to herein as the density profiling system (DPS). The Minnesota Department of Transportation (MnDOT), in particular, has been leading these efforts and improving its DPS system, which is composed of multiple PaveScan antennas, a distance measurement instrument, and a global positioning system antenna receiver.[17] The entire system is easily mounted into a pushcart or a vehicle, as shown in **figure 1**.

FIG. 1

Picture showing vehicle-mounted and cart-mounted DPS systems.

BACKGROUND OF GPR APPLICATIONS FOR ASSESSMENT OF PAVEMENT DENSITY

The GPR makes use of (i) special sensors for transmitting and receiving electromagnetic waves into and from a target structure and (ii) signal processing techniques for extracting certain features that are related to material properties and for detecting anomalies and inclusions in the targeted structure. GPR-based testing methods have found important applications in the pavement industry and are routinely utilized to estimate the layer thicknesses and structural integrity of roadways, as well as to locate covered utilities. Several researchers have proposed various approaches and models for analyzing the GPR signals for different applications. One approach, in particular, the GPR surface reflectivity method has been shown to be suitable for continuous evaluation of the in-place density of asphalt pavements. According to this method, the surface dielectric of the top asphalt mixture layer (ϵ_{AC}) can be derived from

$$\epsilon_{AC} = \left(\frac{1 + \frac{A_o}{A_m}}{1 - \frac{A_o}{A_m}}\right)^2 \tag{1}$$

where A_0 and A_m represent surface reflection amplitudes measured on the pavement surface and on a metal plate, respectively. Testing of the metal plate is carried out at the beginning or at the end of the survey. Subsequently, the ϵ_{AC} values are converted to density using a transfer (calibration) model generated from measured density-dielectric data. From here onward, this model will be referred to as the density-dielectric calibration model.

PROBLEM STATEMENT AND OBJECTIVES

One major challenge to effective implementation of the GPR measurements for pavement density evaluation is establishing a proper density-dielectric calibration curve. Typically, pavement construction projects last several production days (PDs), and asphalt mixtures produced in different PDs may vary considerably. It is in fact for this reason that SHAs and paving contractors make use of an array of QC tools to ensure that the asphalt mixture produced throughout the duration of a project meets the binder content and aggregate quality requirements prescribed in the mix design job mix formula (JMF). Nonetheless, it remains challenging to replicate the exact mix design proportions throughout an entire project. Furthermore, SHAs usually allow contractors to incorporate limited quantities of additives (i.e., mineral filler, antifoaming agents, hydrated lime) or to make small adjustments to the mix design during production. For example, in Minnesota, the plant-produced mixtures are allowed to be within 5 % of the JMF proportions established in the laboratory. In addition, contractors have the option of augmenting the approved JMF with additional sand or rock for a proportion change up to 10 % under specified conditions.[18]

This article investigates the sensitivity of dielectric constants measured by the DPS system to marginal changes in mixture components and explores mix properties that can be employed as triggers for requiring a new calibration

model for converting the dielectric of multiple PDs to density. The study used laboratory-prepared asphalt mixtures with intentionally induced mix proportions changes and plant-produced asphalt mixtures collected on multiple PDs. Gyratory-compacted specimens obtained from these mixtures were tested for density (air void) and subjected to DPS testing. Subsequently, density-dielectric calibration models generated from the test data were compared to assess the appropriateness (or lack thereof) of using a single calibration model for an entire project.

Materials and Methods

The data discussed in this study were primarily obtained from laboratory-prepared and plant-produced asphalt mixtures. Before performing the DPS testing, both loose and gyratory-compacted asphalt mixtures were subjected to routine laboratory tests to determine key material and volumetric properties. The test results were then used to establish the density-dielectric relationships. The following subsections describe the preparation and testing of the asphalt mixtures, as well as the data modeling approach employed in this study.

LABORATORY-MIXED LABORATORY-COMPACTED SPECIMENS

Density and dielectric data collected from MnDOT's MnROAD research facility provided the basis for the laboratory experiments. The MnROAD facility possesses two major roadway segments, mainline and low-volume roads, each containing several dozen approximately 150-m-long test cells. Hoegh et al.[19] obtained GPR-dielectric and bulk density measurements from six test cells with different asphalt mixture types. The researchers found that the cells with mixtures composed primarily of limestone, a higher dielectric aggregate source, resulted in a higher dielectric profile than the cells with mixtures composed primarily of granite. As shown in **figure 2**, data from all the test cells not containing limestone fall close to a common density-dielectric curve, whereas data from test cells constructed using asphalt mixtures containing significant limestone shifted significantly to the right. Other mix characteristics appeared to have lesser impact.

Based on this observation a laboratory experimental testing plan was developed in such a manner to evaluate and quantify the effects of limestone by progressively increasing its content in a control mix design. A MnDOT approved, level III Superpave 19 mm mix design was considered as a baseline for developing the mixtures for the study. The mix design called for use of three virgin aggregates and the recycled asphalt pavement (RAP) described in **Table 1**.

The aggregates in **Table 1** were sampled and used to prepare four aggregate gradation blends, one of which was an exact replication of the original mix design (AS0), and the other three were obtained by making changes to the mix design proportions (AS1, AS2, and AS3). The amount of limestone-sand (L-sand) in the aggregate blends

FIG. 2

Density-dielectric relationships of MnROAD tests cells.

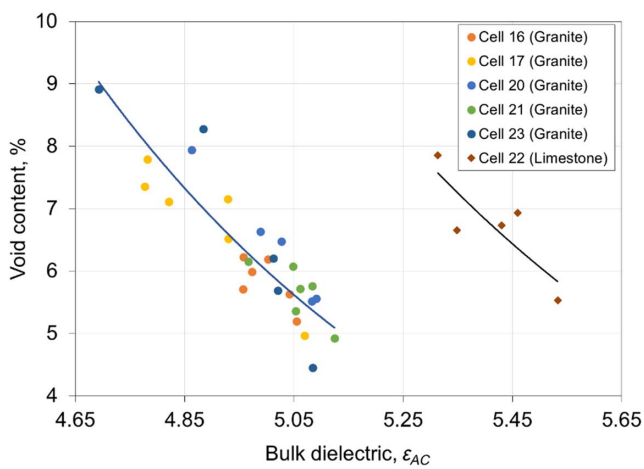

TABLE 1
Aggregates used to prepare the laboratory asphalt mixtures

Aggregate Source	ID	Type	Minus #4	Gsb, g/cm^3
McCrossan Maple Grove 3/4" rock	Ba-rock	Rock	2 %	2.681
McCrossan Maple Grove 3/8" rock	…	Rock	31 %	2.653
Kraemer Burnsville 1" clear	1-in. Limechip	Limestone	4 %	2.654
Kraemer Burnsville 3/8" clear	3/8 l-Chips	Limestone	29 %	2.656
Kraemer lime-sand clear	L-Sand	Limestone	97 %	2.652
Martin Marietta St. Cloud washed sand	G-Sand	Granite	99 %	2.655
McCrossan Rap	Rap	Rap	74 %	2.648

was gradually increased from 13 to 33 % by replacing portions of the granite-sand and the RAP material as summarized in figure 3. The three aggregates selected for the modifications, shown in figure 4, were similar in size and thus the changes did not affect the gradations.

The gradation curves of the laboratory-prepared aggregate blends, shown in figure 5 (0.45 power charts), depicted four dense and similar aggregate gradations. This occurrence effectively removed a critical source of variability (gradation) and made it easier to concentrate on the effects of mixture components' type and origin.

The four aggregate structures were then mixed with a PG 58-28 asphalt binder, at rates close to the optimum value reported in the original JMF, to prepare the four asphalt mixtures. The asphalt mixture obtained from the

FIG. 3
Summary of aggregate blends prepared used for the laboratory mixtures.

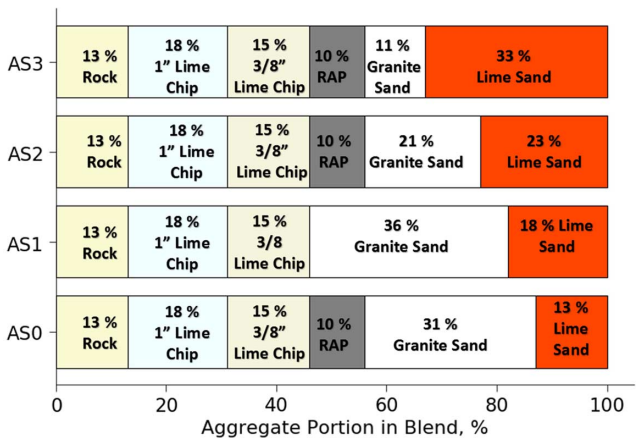

FIG. 4
Pictures of the aggregate selected for mix design modifications.

FIG. 5

Aggregate gradations of the laboratory-prepared mixtures.

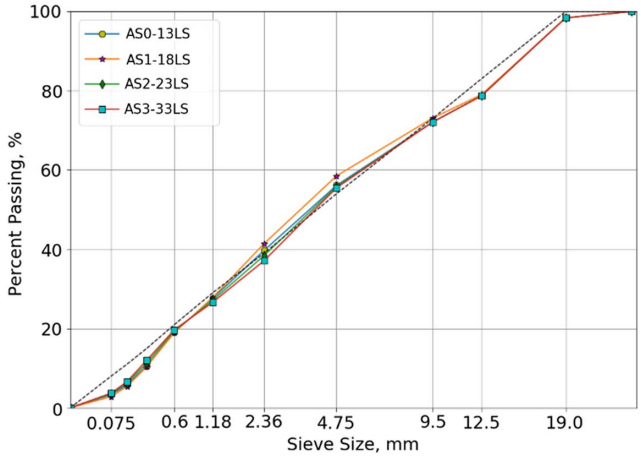

AS1 blend (without RAP) turned out to be dryer than the remaining mixtures, and thus it did not achieve similar levels of air void contents (under the same compaction effort) as the others.

Table 2 reports the relevant material properties of the mixtures. The mix proportion modifications resulted in significant changes to the asphalt mixture properties. In particular, the maximum specific gravity (G_{mm}) of the loose mixtures increased almost linearly with the increase of limestone sand (Lime-Sand). On the contrary, the effective asphalt binder decreased with the amount of limestone content. The fine-to-effective binder ratio and the absorbed asphalt binder also increased slightly with the increase of limestone, but remained below one.

Consecutively, the asphalt mixtures were compacted into 150-mm-diameter by 110±5-mm-height cylinders at three different target air void contents using a Superpave gyratory compactor (SGC). The amount of material placed in the SGC molds was adjusted to achieve the desired target air void contents while maintaining the geometry of the finished specimens. For each asphalt mixture, a total of 9 specimens with three replicates for each level of air void contents, were fabricated. Afterward, the bulk specific gravity (G_{mb}) of the compacted specimens was determined using a CoreLok vacuum chamber.[20] The CoreLok was preferred to ensure that the specimens did not get into contact with water prior to the DPS testing. After the DPS testing, which is discussed

TABLE 2

Key mix properties of the asphalt mixtures considered in the study

	Laboratory Mixtures				Field Mixtures	
Mix Property	AS0-13LS-28	AS1-18LS-28	AS2-23LS-28	AS3-33LS-28	MN-TH371	AL-Glenn Hwy
NMAS	19 mm	19 mm	19 mm	19 mm	12.5 mm	12.5 mm
PG	58-28	58-28	58-28	58-28	58H-34	64-40
Gsb	2.657	2.658	2.657	2.657	2.646	2.708
Pb	5.1	5.2	4.8	4.8	5.1	5.4
F/Pbe	0.7	0.6	0.8	0.9	0.8	1.1
Gmm	2.484	2.495	2.509	2.511	2.469	2.515
Gse	2.688	2.706	2.705	2.708	2.679	2.751
Pba	0.4	0.7	0.7	0.7	0.5	0.6
Pbe	4.7	4.5	4.1	4.1	4.6	4.8

Note: F/Pbe = ratio of fines to effective binder; Gmm = maximum specific gravity of asphalt mixtures (g/cm^3); Gsb = bulk specific gravity of the aggregate blend (g/cm^3); Gse = effective specific gravity of aggregate (g/cm^3); NMAS = nominal maximum aggregate size; Pb = asphalt binder content (%); Pba = absorbed asphalt binder (%); Pbe = effective asphalt binder (%).

next, the specimens were retested according to the saturated surface dry method[21] to ensure the two density determination methods yielded similar G_{mb} values. The air void content (V_a) is computed using equation (2).

$$V_A = 100 \times \frac{G_{mm} - G_{mb}}{G_{mm}} \tag{2}$$

The measurement of dielectric on the specimens was carried out using the concept of time-of-flight (TOF) method, which was further improved by GSSI Inc. and MnDOT[22] to isolate sufficiently the surface reflections from the direct coupling, edge diffractions, and multiple reflection signals. These improvements enabled accurate measurements of dielectric from gyratory-compacted specimens. The details of the test procedure and the TOF methodology were beyond the scope of this article and are articulated in a companion article.

PLANT-MIXED LABORATORY-COMPACTED (PMLC) SPECIMENS

One primary reason for including plant-produced asphalt mixtures in this study was to check whether the day per day production variability alone would affect the density-dielectric relationship to such an extent that a single calibration model would not be sufficient to evaluate a project. Another reason was to assess the ability of the analytical model used in this study to characterize field asphalt mixtures that were considerably different from the ones used in the laboratory experiments. The plant-produced mixtures available for this study were composed of aggregates and asphalt binders different from the ones used in the laboratory setup, and they were produced in a less-controlled environment (plant-produced) on several PDs. The gradation curves of the plant-produced mixtures are shown in figure 6.

Highway 371, Hackensack, Minnesota

The wearing coarse mixture used in this project consisted of a level III Superpave 12.5-mm mix prepared using a PG 58H-34 binder. Samples of loose asphalt mixture, collected from multiple PDs between September 29 and October 4, 2018, were collected and compacted in the laboratory at different air void levels. Portions of the sampled material were utilized to determine material properties of the loose asphalt mixtures. The compacted specimens were then subjected to GPR and density testing as described previously.

Glenn Highway: Hiland to Ektulna, Alaska

The mixture used for this project comprised a highly modified asphalt binder PG 64-40 and a local hard-aggregate source classified as diorite. The mixture also contained 15 % RAP and made use of warm-mix antistrip additive Evotherm P-25. The paving project took place during 22 days of paving from May 22 to June 23, 2017.

FIG. 6

Aggregate gradations of the plant-produced mixtures.

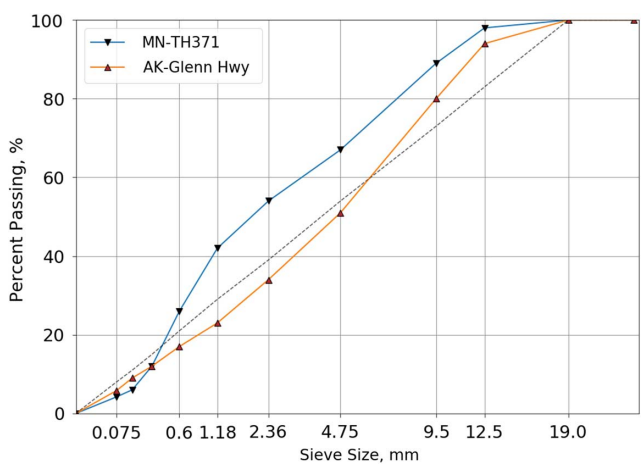

The GPR-dielectric values, in this case, were measured directly on the new pavement on randomly selected spots. After taking the GPR readings, the marked locations were cored and tested in the laboratory for bulk density. G_{mm} was determined on one bulk sample per 5,000-ton lot of asphalt. The bulk samples were taken from the windrow of asphalt mixture deposited on grade by belly dumps just ahead of the paving train. The lot G_{mm} was used for calculation of percent compaction for the ten cores drilled from that lot of asphalt mixture.

DATA PROCESSING AND MODELING

Current approaches for converting dielectric to density rely on simple linear or exponential[19] empirical relationships. The major disadvantage of these relationships is that they lack material (mix) characteristics that may be useful for a compelling mix sensitivity study. Fortunately, the literature review provided several mixture-characteristic–dependent models that can be used to express the density-dielectric relationship. One of these models, the Al-Qadi et al.[13] referred to as the Al-Qadi Lahouar Leng (ALL) model, was found to fit the data generated in this study very well. The ALL-model is described in equation (3):

$$G_{mb} = \frac{\frac{E_{AC}-E_B}{3E_{AC}-2.3E_B} - \frac{1-E_B}{1+2E_{AC}-2.3E_B}}{\left(\frac{E_S-E_B}{E_S+2E_{AC}-2.3E_B}\right)\left(\frac{1-P_b}{G_{se}}\right) - \left(\frac{1-E_B}{1+2E_{AC}-2.3E_B}\right)\left(\frac{1}{G_{mm}}\right)} \tag{3}$$

where ϵ_B and ϵ_s provide information regarding the dielectrics of asphalt binder and the overall aggregate structure, respectively. The remaining variables of equation (3) are mixture components reported in Tables 2 and 3. In this study, ϵ_B and ϵ_s were back-calculated using a nonlinear optimization technique within specified physical bounds: from 2 to 3 and from 4 to 8 for the ϵ_B and ϵ_s, respectively. The bulk density can be converted to air void content using equation (2). It should be noted that there exist several mixing-theory–based models; however, the ALL-model has been found to provide the best density predictions from GPR readings.[15]

Results and Discussions

A curve-fitting approach based on nonlinear least-squares minimization was used to fit the ALL-model (equation (3)) to the density and dielectric data. The mix parameters, G_{mm}, G_{se}, and P_b were those from the mix design reports, whereas the aggregate and binder dielectric constants, ϵ_s and ϵ_b, respectively, were obtained by the optimization process and adjusted so that the ALL-model matches the data closely. All data fitted well to the ALL-model curves generated using the input parameters in Table 3.

RESULTS OF THE LABORATORY-PRODUCED MIXTURES

In the four laboratory mixtures, the back-calculated binder parameter values were the same. This was an expected outcome because the four mixtures used the same binder. On the contrary, the aggregate parameter ϵ_S varied considerably among the mixtures. Hence, noting that all these mixtures possessed similar gradation curves and

TABLE 3
Back-calculated ALL-model input parameters

	Laboratory-Prepared Mixtures				Plant-Produced Mixtures				
Input	AS0-13LS	AS1-18LS	AS2-23LS	AS3-33LS	371-29	371-01	371-02	371-04	Glenn Hwy.
G_{mm}	2.484	2.495	2.509	2.511	2.476	2.472	2.476	2.469	2.576
P_b	5.2	5.2	4.9	4.9	5.1	5.2	5.0	5.0	5.4
G_{se}	2.688	2.706	2.705	2.708	2.679	2.678	2.674	2.666	2.751
ϵ_S	6.38	6.54	6.57	6.72	5.92	5.77	5.83	5.77	6.15
ϵ_b	2.0	2.0	2.0	2.0	2.0	2.0	2.0	2.0	3.0
$R^2_{adj.}$	0.97	0.96	0.97	0.97	0.86	0.91	0.94	0.92	0.91

particle sizes, the variations were attributed primarily to the different contents of limestone: ϵ_S increased as the limestone content increased. This observation implies that the ϵ_S parameter should be considered as a bulk value associated with a specific gradation and aggregate distribution.

Figures 7 and 8 show the density-dielectric and void-dielectric relationships of the mixtures, respectively. The continuous lines represent the fitted ALL-model curves. Accordingly, the density-dielectric curves of the mixtures shifted from top-left to bottom-right (almost linearly) for increasing limestone content (13 to 33 %). The mixture without RAP (AS1-18LS-28) also respected this trend, although in a less marked manner. Figure 8 shows that the void-dielectric curves shifted from bottom-left to top-right for increasing limestone content.

RESULTS OF THE PLANT-PRODUCED MIXTURES

The four production mixture data sets from TH 371 fit the ALL-model very well. The TH371 data exhibited higher variability than the mixtures prepared in the laboratory and contained several noticeable outliers that were removed from the analyses. Figure 9 indicates that the curves from the four different PDs were reasonably close. It can be argued that any of these curves, used for the conversion of the dielectric to density, would have provided an estimate of the voids within 1 % of accuracy. The binder dielectric back-calculated from the PG 58-34

FIG. 7

Density-dielectric relationships of the laboratory mixtures.

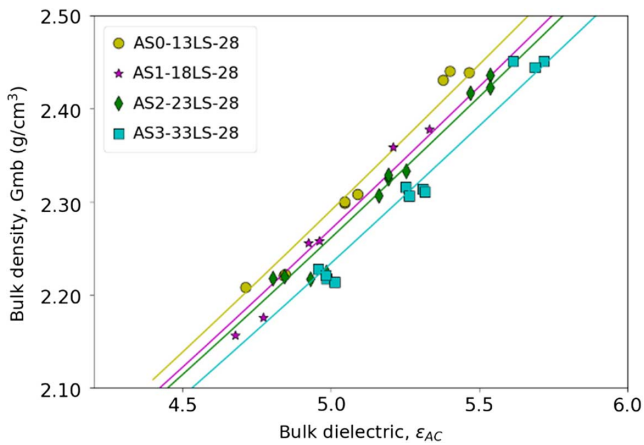

FIG. 8

Void-dielectric relationships of the laboratory mixtures.

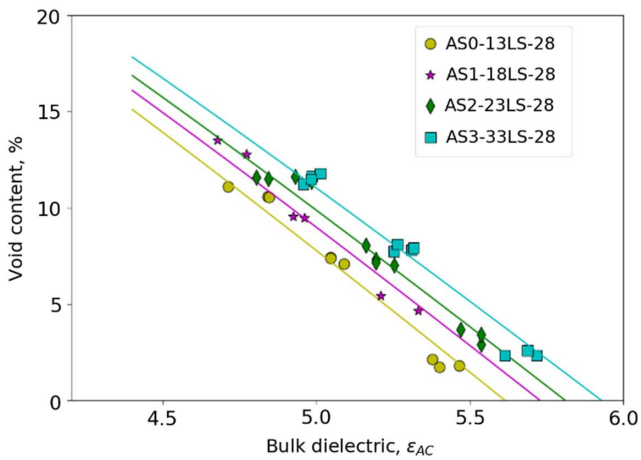

FIG. 9

Density-dielectric relationships for the plant mixtures from MN-TH371.

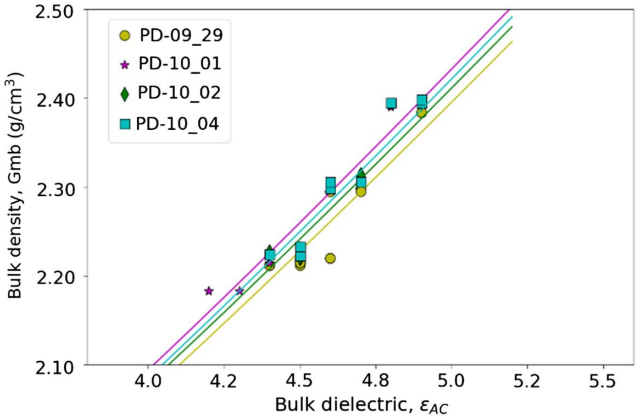

FIG. 10

Density-dielectric relationships for the plant mixture from Glenn Hwy., Alaska.

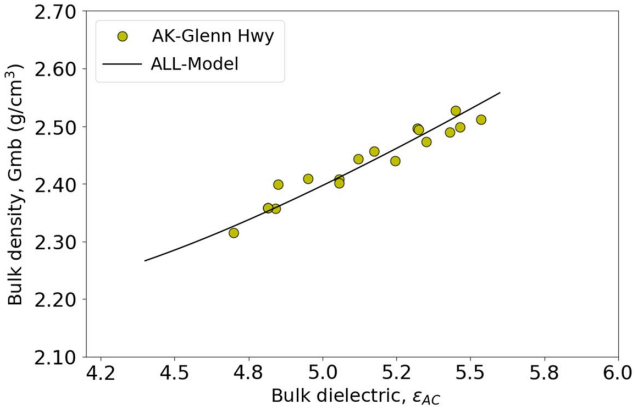

binder used in the TH371 mixtures was the same as the one calculated for the PG58-28 used in the laboratory-prepared mixtures, suggesting that the two binders had a similar effect on the compatibility of the mixes.

On the contrary, the ϵ_b calculated from the Alaskan project data, shown in figure 10, was larger than the others, reflecting the significantly different material properties of a PG 64-40 binder as compared to the PG 58-28 and PG 58-34 binders.

The aggregate parameter values of the TH371 mixtures were similar to each other but notably lower than the ones derived for the laboratory mixtures. The difference may be explained in part by the difference in gradations and particle sizes. The aggregate parameter of the Alaskan mixture, composed primarily of diorite aggregate, was similar to values observed for the Minnesotan laboratory mixtures.

DISCUSSION AND ANALYSIS OF RESULTS

The material-dependent model was particularly suitable for investigating the effects of mixture variability on GPR readings, as elaborated in what follows.

Effect of Limestone Content

A quantitative estimate of the effect of increasing the limestone content in an asphalt mixture can be obtained using equation (3) and the model input parameters derived from the laboratory prepared mixes, as shown in

FIG. 11

Plot showing effects of increasing limestone on void content of asphalt mixtures.

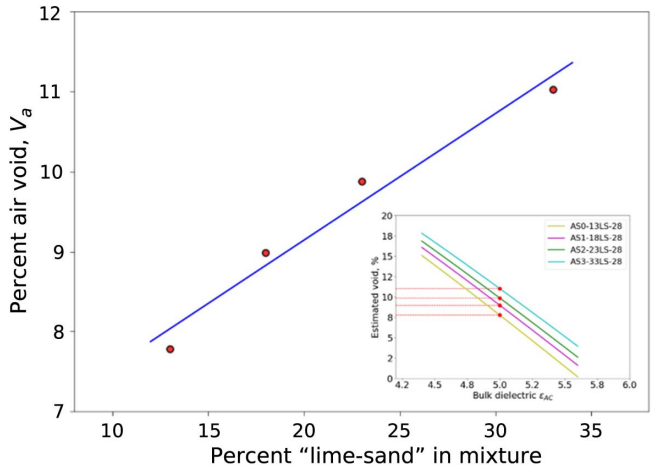

figure 11. The figure shows differences in estimated air void contents of the four mixtures for a specified dielectric constant. Accordingly, the densities and void contents associated with a fixed dielectric value were calculated for the four laboratory mixtures. Based on this type of analysis, it was observed that for the same levels of compaction, gradation, and binder content, the mixtures with a higher content of lime-sand yielded higher air void content: the rate of air void increase was estimated at 0.2 % for every percent of lime-sand added. Consequently, if the calibration model obtained from the AS0-13LS-28 mixture was used to convert the GPR-dielectrics measured on the AS3-33LS-28 mixture, the actual void contents would have been underestimated by about 4 %. The implication of this observation in interpreting GPR readings for compaction evaluation is that mix adjustments during construction (for example, adding or replacing certain components of the mixture) has a significant effect on the dielectric measurement. Therefore, adjustments should be confined or restricted. Alternatively, new dielectric-density calibration models should be required for every field adjustment. For example, based on the rate estimated in this study, in order to ensure an accuracy of 1 % in the air void predictions, recalibration should be required for every field adjustment above 1 % of an aggregate source.

Potential Asphalt Mix Property for Requiring Recalibration

The previous findings indicate that a new dielectric-density calibration model should be required for field adjustment deemed significant enough to affect the curve relating dielectric to air voids. To this end, sensitivity studies similar to that presented in this article can be used to build a database determining thresholds for changes to the different mix components that should trigger asphalt sample dielectric testing or model recalibration. The fundamental understanding of the effect of mixture changes on dielectric readings from mixture sensitivity evaluation is critical to reducing excessive field testing that may be an impediment to implementation.

Advanced Mixture Sensitivity Study

The ALL-model was further employed to perform qualitative sensitivity analyses aimed at identifying the mix characteristics that contribute the most to variation in density (or air void) of asphalt pavements. A global sensitivity analysis (GSA) method was performed using equation (4) to evaluate the contribution of each input parameter as well as their interactions to the overall variance of the model output, G_{mb}:

$$G_{mb} = f(\epsilon_{AC}, \epsilon_B, \epsilon_S, G_{mm}, P_b) \tag{4}$$

As can be seen by comparing equations (3) and (4), the G_{se} input parameter was redefined in the function of the other two mix parameters, G_{mm} and P_b, and removed from equation (4). This modification was necessary to

TABLE 4
Typical range of variations for the ALL-Model input parameters

Input	Description	Unit	Typical Ranges
ϵ_{AC}	Dielectric of asphalt mixture (bulk)	…	3.0–6.0
ϵ_S	Dielectric of the aggregate structure	…	5.0–9.0
ϵ_B	Dielectric of the asphalt binder	…	2.0–3.0
Pb	Asphalt binder content	%	4.0–8.0
G_{mm}	Maximum Specific gravity of asphalt mixture	g/cm^3	2.300–2.700
G_{se}	Aggregate effective specific gravity	g/cm^3	2.500–3.000

ensure the independence of the input variables (a prerequisite for statistical analyses). The GSA sensitivity analysis methods consist of varying all the model input parameters at the same time and in performing statistical evaluations of their output. However, because it is generally impractical to evaluate all the possible combinations of the input variables, Monte-Carlo–based sampling algorithms are typically used to generate more or less dense sequences of quasirandomly distributed input parameters within predefined ranges of variation (see **Table 4**). The specific GSA technique used in this study was a Monte-Carlo–based analysis technique called the "Saltelli-Sobol method," which is offered in the SALib package library in python.[23] The input parameters and their range of variations are reported in **Table 4**.

The Saltelli sampling technique generated more than 700,000 sequences of $\epsilon_{AC}, \epsilon_B, \epsilon_S, G_{mm}, P_b$ that were used to feed the model in equation (4) and compute the bulk density. The density values were then converted into air void content using equation (2). This approach generated a sufficiently dense and reasonable approximation of real air void contents, as illustrated in the histogram shown in **figure 12**. The combination of input parameters that yielded air voids content below 1 % (physically not realistic) represented only 7 % of the total number of output used for the variance analysis.

The second part of the SALib package was used to perform Sobol analysis on the model output: decomposition of the output variance into terms attributable to each input parameter (main effect) and the interaction between the parameters (higher-order interactions). The precise details of the Sobol analysis and indices are discussed elsewhere.[24] For this article, it is sufficient to recall that the method decomposes the variance of the model output $Var(G_{mb})$ into the contribution associated with each input parameter or with the interaction between multiple input parameters. The method then provides the following indices: (i) first-order effect (S_i) quantifying the effect of a single parameter on $Var(G_{mb})$; (ii) total effect (S_T), which comprises the first-order effect and all the interaction effects involving a specific parameter; and (iii) second-order interaction (S_{ij}) expressing the amount of variance of G_{mb} explained by the interaction of two inputs. Indices for higher than two

FIG. 12
Histogram of simulated void contents from the Saltelli-sampled sequences.

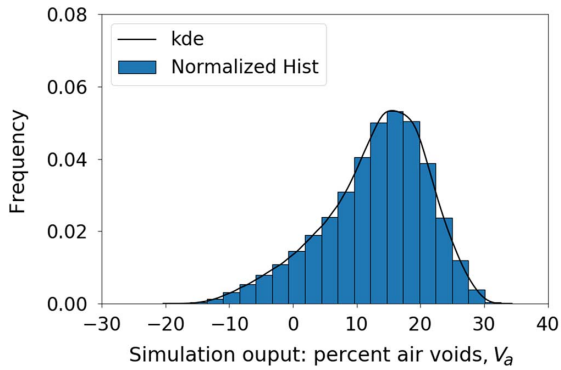

interactions are generally unpractical and difficult to interpret. The individual (S_i), total (S_T), and second-order interaction (S_{ij}) sensitivity indices sorted in order of significance are reported in figures 13–15.

Based on the previous analysis, the two most important factors affecting the density outputs were the dielectrics of the aggregate structure and the asphalt mixture. The other material parameters, and in particular the binder content, had a lesser impact. The relationship of G_{mm} to density and air void were found to be significant within narrow ranges, thus mixture specific. Overall, only the main effects of the input parameters were found significant; the higher-order interactions were negligible.

FIG. 13

Sobol-Saltelli first-order sensitivity indices for the ALL-model.

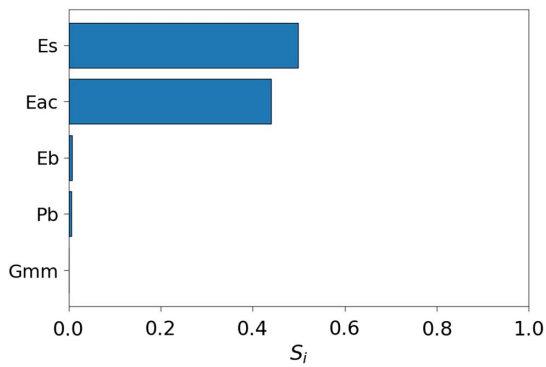

FIG. 14

Sobol-Saltelli total effects sensitivity indices for the ALL-model.

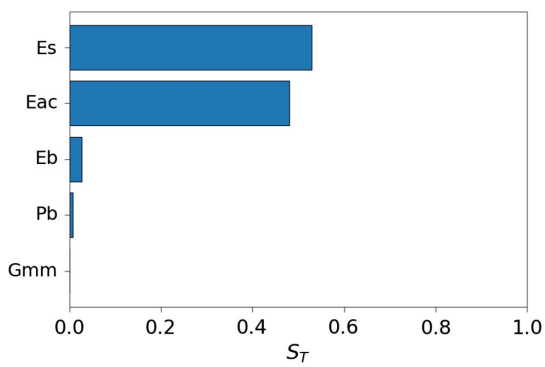

FIG. 15

Sobol-Saltelli second-order interaction sensitivity indices for the ALL-model.

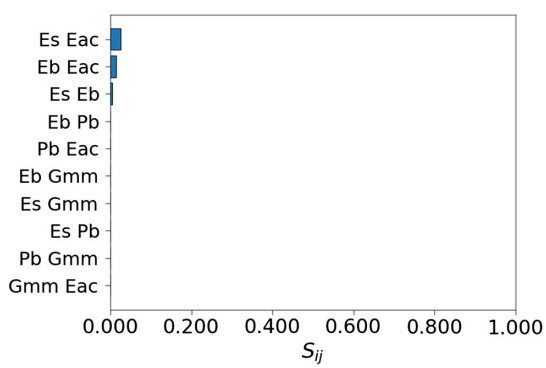

FIG. 16

Sobol-Saltelli simulation outputs: void versus mixture dielectric (ϵ_{ac}).

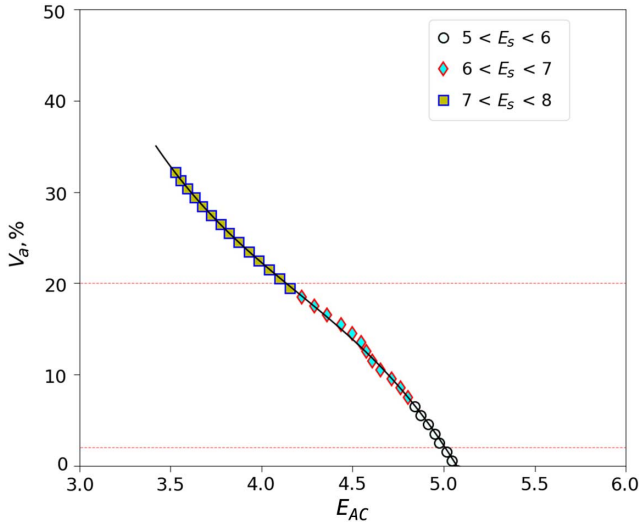

FIG. 17

Sobol-Saltelli simulation outputs: void versus aggregate dielectric (ϵ_s).

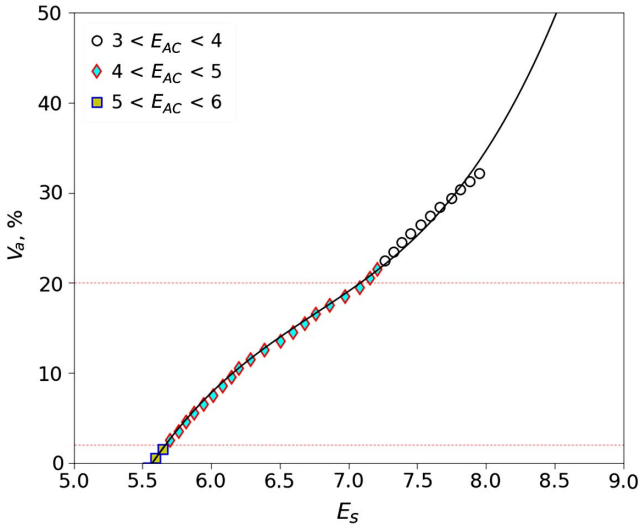

The data generated in the analyses were also rearranged and displayed as in figures 16 and 17 to draw further observations on the effect of the two main input parameters: ϵ_{ac} and ϵ_s. In figure 16, the simulated ϵ_{ac} are plotted against the void contents for different ranges of ϵ_s. In figure 17, ϵ_s are plotted against the void contents for different ranges of ϵ_{ac}. The information in these plots can be summarized as follows: for similar compaction efforts, high asphalt mixture dielectric readings would indicate low air void values, whereas high aggregate dielectric values will result in higher air voids.

Summary of Findings and Recommendations

This article discussed the importance, recent advances, and challenges in using GPR technologies for rapid, full-coverage, and nondestructive evaluation of compaction in newly constructed asphalt pavements. The dielectric

measurements from GPR on the pavement surface can be converted to compaction density using density-dielectric calibration models generated from the same asphalt mixture used to construct the roadway. However, the production and construction variability of asphalt mixtures and the practices of field adjustments to mix design have great effects on the appropriateness and accuracy of the calibration models. Therefore, the study presented herein aimed at investigating the sensitivity of dielectric measurements of the DPS system to marginal changes in mix components. Experimental testing, including material characterization, density determination, and GPR scanning, were performed on laboratory-prepared and plant-produced asphalt mixtures. The Al-Qadi, Lahouar, and Leng (ALL-model), a material-dependent model, was found suitable for analyzing the data generated in this study and for performing more advanced statistical sensitivity analyses. Some of the main findings and recommendations that were drawn from this study can be summarized as follows:

- The laboratory experiments were specifically designed to isolate and evaluate the impact of limestone in asphalt mixtures on the density-dielectric relationship. The amount of limestone-sand in the aggregate blends was gradually increased to replace portions of granite-sand and RAP materials of similar particle size. As a result, the gradation curves of the aggregate blends prepared in the laboratory were all alike. Furthermore, the mixtures were blended using the same asphalt binder grade and content. Testing conducted on gyratory-compacted specimens obtained from these mixtures confirmed that dielectric constants of mixtures are particularly sensitive to dielectrics of aggregates such as limestone. For example, even small changes in the content of the limestone source appeared to affect the density-dielectric relationships considerably. The results showed that a percent increase in limestone while maintaining all other factors (i.e., gradation, binder content, compaction level) intact would result in approximately 0.2 percent increase in air void content.
- Plant-produced asphalt mixtures sampled from multiple PDs were employed to assess the impact of production variability on the dielectric constant. The variability between mixes from different PDs (originated from the same mix design) did not appear to be large enough to warrant more than one density-dielectric calibration model. Noting that generating a large number of calibration models for a single project is costly, not feasible, and probably unnecessary; it would be reasonable to rely on a single calibration model as long as the aggregate source proportions are maintained intact.
- The aggregate source/composition was found to be the factor that most affects the density-dielectric relationships of asphalt pavements. Asphalt mixtures containing high-dielectric aggregate source will result in higher air void content (lower density) than mixtures with a lower-dielectric aggregate source for similar compaction efforts
- Understanding that the dielectric-density relationships are particularly sensitive to the aggregate source and gradation, it is recommended that highway agencies restrict mix design adjustments during construction that include adding new aggregate sources. Alternatively, they should require new dielectric-density calibration models for every field adjustment or when a significant discrepancy in G_{mm} has registered.
- Ongoing and future works will focus on evaluating how the difference between laboratory-prepared and plant-produced mixture impact the density-dielectric relationships.

ACKNOWLEDGMENTS

This article is based upon work partially supported by the Federal Highway Administration (FHWA)'s SHRP2 Solutions (funding program code M6T0) and the Minnesota Department of Transportation (MnDOT)'s Materials and Road Research programs. The authors gratefully acknowledge the support. However, the findings, opinions, and recommendations expressed in this publication are those of the authors and do not necessarily reflect the views of the FHWA or MnDOT. The authors gratefully acknowledge the valuable assistance of Debra Evans and Ray Betts (MnDOT Bituminous Office) in the development and preparation of the laboratory mixtures. The authors are also thankful to Jeff Brunner and Glenn Engstrom for their technical assistance and managerial oversight and their continuous support of research on innovative technologies.

References

1. C. S. Hughes, *Compaction of Asphalt Pavement, National Cooperative Highway Research Program Synthesis of Highway Practice 152* (Washington, DC: Transportation Research Board, 1989).
2. J. A. Epps, C. L. Monismith, W. B. Warden, P. S. Pell, B. F. Kallas, R. L. Terrell, H. W. Busching, and N. W. McLeod, "Influence of Mixture Variables on the Flexural Fatigue Properties of Asphalt Concrete," in *Association of Asphalt Paving Technologists* (White Bear Lake, MN: Association of Asphalt Paving Technologists, 1969), 423–464.
3. J. T. Harvey and B.-W. Tsai, "Effects of Asphalt Content and Air Void Content on Mix Fatigue and Stiffness," *Transportation Research Record* 1543, no. 1 (January 1996): 38–45. https://doi.org/10.1177/0361198196154300105
4. S. B. Seeds, R. G. Hicks, G. E. Elkins, H. Zhou, and T. V. Scholz, *LTTP Data Analysis: Significance of "As-Constructed" AC Air Voids to Pavement Performance, NCHRP Project 20-50(14)* (Washington, DC: Transportation Research Board, 2002).
5. P. B. Blankenship and R. M. Anderson, "Laboratory Investigation of HMA Modulus, Flow Number and Flexural Fatigue on Samples of Varying Density," *Journal of the Association of Asphalt Paving Technologists* 79 (2010): 497–518.
6. H. Wang, Z. Wang, T. Bennert, and R Weed, *HMA Pay Adjustment, FHWA NJ-2015-007* (Trenton, NJ: New Jersey Department of Transportation, 2015).
7. F. Beainy, S. Commuri, and M. Zaman, "Quality Assurance of Hot Mix Asphalt Pavements Using the Intelligent Asphalt Compaction Analyzer," *Journal of Construction Engineering and Management* 138, no. 2 (February 2012): 178–187. https://doi.org/10.1061/(ASCE)CO.1943-7862.0000420
8. F. L. Roberts, P. S. Kandhal, E. R. Brown, D.-Y. Lee, and T. W. Kennedy, *Hot Mix Asphalt Materials, Mixture Design and Construction* (Lanham, MD: National Asphalt Paving Association Education Foundation, 1996).
9. V. L. Gallivan, G. K. Chang, and R. D. Horan, "Practical Implementation of Intelligent Compaction Technology in Hot Mix Asphalt Pavements," *Journal of the Association of Asphalt Paving Technologists* 80 (2011): 1–32.
10. R. L. Lytton. System identification and analysis of subsurface radar signals. U.S. Patent 5,384,715, filed August 27, 1993, and issued January 24, 1995.
11. T. Saarenketo, "Using Ground-Penetrating Radar and Dielectric Probe Measurements in Pavement Density Quality Control," *Transportation Research Record* 1575 (January 1997): 34–41. https://doi.org/10.3141/1575-05
12. T. Saarenketo and T. Scullion, "Road Evaluation with Ground Penetrating Radar," *Journal of Applied Geophysics* 43, nos. 2–4 (March 2000): 119–138. https://doi.org/10.1016/S0926-9851(99)00052-X
13. I. L. Al-Qadi, Z. Leng, S. Lahouar, and J. Baek, "In-Place Hot-Mix Asphalt Density Estimation Using Ground-Penetrating Radar," *Transportation Research Record* 2152 (January 2010): 19–27. https://doi.org/10.3141/2152-03
14. P. Georgiou and F. Loizos, "Assessment of In-Situ Compaction Degree of HMA Pavement Surface Layers Using GPR and Novel Dielectric Properties-Based Algorithms" (paper presentation, European Geosciences Union General Assembly, Vienna, Austria, April 12–17, 2015).
15. C. Plati, P. Georgiou, and A. Loizos, "A Comprehensive Approach for the Assessment of HMA Compactability Using GPR Technique," *Near Surface Geophysics* 14, no. 2 (April 2016): 117–126. https://doi.org/10.3997/1873-0604.2015043
16. L. Khazanovich, K. Hoegh, R. Conway, and S. Dai, *SHRP2 Solutions: Nondestructive Evaluation of Bituminuos Compaction Uniformity Using Rolling Density* (St. Paul, MN: Minnesota Department of Transportation, 2017).
17. *Standard Practices for Asphalt Surface Dielectric Profiling System Using Ground Penetrating Radar*, AASHTO PP 98-19 (Washington, DC: American Association of State Highway and Transportation Officials, 2019).
18. Minnesota Department of Transportation, *Standard Specifications for Construction* (St. Paul, MN: Minnesota Department of Transportation, 2018).
19. K. Hoegh, S. Dai, T. Steiner, and L. Khazanovich, "Enhanced Model for Continuous Dielectric-Based Asphalt Compaction Evaluation," *Transportation Research Record* 2672, no. 26 (September 2018): 144–154. https://doi.org/10.1177/0361198118794068
20. *Standard Method of Test for Percent Air Voids in Compacted Dense and Open Asphalt Mixture*, AASHTO T 269 (Washington, DC: American Association of State Highway and Transportation Officials, 2018).
21. *Standard Method of Test for Bulk Specific Gravity (Gmb) of Compacted Hot Mix Asphalt (HMA) Using Saturated Surface-Dry Specimens*, AASHTO T 166 (Washington, DC: American Association of State Highway and Transportation Officials, 2016).
22. K. Hoegh, R. Roberts, S. Dai, and E. Zegeye Teshale, "Toward Core-Free Pavement Compaction Evaluation: An Innovative Method Relating Asphalt Permittivity to Density," *Geosciences* 9, no. 7 (June 2019): 280. https://doi.org/10.3390/geosciences9070280
23. J. Herman, W. Usher, C. Mutel, B. Trindade, D. Hadka, M. Woodruff, F. Rios, and D. Hyams, "SALib - Sensitivity Analysis Library in Python," SALib, 2019. http://web.archive.org/web/20200121054827/https://salib.readthedocs.io/en/latest/
24. A. Saltelli, M. Ratto, T. Andres, F. Campolongo, J. Cariboni, D. Gatelli, M. Saisana, and S. Tarantola, *Global Sensitivity Analysis: The Primer* (Chichester, UK: Wiley & Sons, Ltd, 2008)